

Amplitude scaling of asymmetry-induced transport in a non-neutral plasma trap

D. L. Eggleston and B. Carrillo

Occidental College, Physics Department, Los Angeles, California 90041

(Received 19 September 2001; accepted 28 November 2001)

Initial experiments on asymmetry-induced transport in the Occidental non-neutral plasma trap found the radial particle flux at small radii to be proportional to ϕ_a^2 , where ϕ_a is the applied asymmetry amplitude. Other researchers, however, using the global expansion rate as a measure of the transport, have observed a ϕ_a^1 scaling when the rigidity (the ratio of the axial bounce frequency to the azimuthal rotation frequency) is in the range of 1–10. In an effort to resolve this discrepancy, measurements have been extended to different radii and asymmetry frequencies. Although the results to date are generally in agreement with those previously reported (ϕ_a^2 scaling at low asymmetry amplitudes falling off to a weaker scaling at higher amplitudes), some cases have been observed where the low amplitude scaling is closer to ϕ_a^1 . Both the ϕ_a^2 and ϕ_a^1 cases, however, have rigidities less than 10. Instead, the ϕ_a^1 cases are characterized by an induced flux that is comparable in magnitude but opposite in sign to the background flux. This suggests that the mixing of applied and background asymmetries plays an important role in determining the amplitude scaling of this transport. © 2002 American Institute of Physics. [DOI: 10.1063/1.1436493]

I. INTRODUCTION

Malmberg–Penning traps are now being used in a variety of experiments. Understanding the properties of these traps is thus of considerable practical as well as fundamental interest. It has long been known that the confinement in Malmberg–Penning traps is limited by the presence of asymmetric electric and magnetic fields. Early confinement studies found that at low neutral pressures the confinement time was much less than expected from transport due to electron-neutral collisions.¹ It was suggested that this anomalous transport was due to the presence of electric or magnetic fields that break the cylindrical symmetry of the trap. The presence of such asymmetries would produce a radial component to the $E \times B$ or ∇B drift that would lead to particle loss to the walls of the trap. This suggestion led to a number of experiments^{2–8} employing *applied* asymmetries in order to study the transport in a controlled manner. Most of the experiments have used electric asymmetries since these are easily applied and manipulated using the sectored wall portions of the confinement region of the trap.

A basic issue of asymmetry-induced transport is the scaling of the transport with asymmetry amplitude. Current theory⁹ predicts two transport regimes depending on the amplitude of the asymmetry potential in the plasma ϕ . For smaller amplitudes (the plateau regime), the radial flux Γ is proportional to the square of the asymmetry potential ϕ^2 . For larger amplitudes (the banana regime), the flux scales like the square root of the asymmetry potential $\phi^{1/2}$.

Previous experiments on amplitude scaling have used a variety of measures to characterize the transport and have applied the asymmetries in different ways. Notte and Fajans³ applied a switched dc voltage to a 50 degree wall patch in the central part of the confinement region. Following earlier work, they measured the time τ_m for the central density to

decrease by one-half and found that this confinement time scaled like ϕ_a^{-m} with $1.7 < m < 2.1$. This scaling roughly agrees with plateau-regime scaling, although the voltages used in this experiment (up to 40 volts) would seem to be much too high to satisfy the plateau regime requirement.

More recently, Kriesel and Driscoll^{6–8} have employed switched dc voltages applied at the end of the plasma column to study this transport over a wide range of parameters. For most of these experiments they used the rate of change of the mean-square-radius $\Delta \nu$ (with the background rate subtracted off) to characterize the transport. They found two transport regimes determined by the experimental value of the rigidity, which is the ratio of the axial bounce frequency to the azimuthal rotation frequency. When the rigidity was between 1 and 10, the expansion rate $\Delta \nu$ scaled like ϕ_a^1 , whereas higher values of rigidity gave a ϕ_a^2 scaling.

Our earlier studies⁵ in a modified trap (described below) found that the time rate of change of the plasma density dn/dt (measured at one radius) scaled like $\phi_a^{2.1}$ for small asymmetry amplitudes and like $\phi_a^{1.3}$ for larger amplitudes. The radial flux Γ was found to have a similar scaling. The rigidity for these measurements was small (approximately 0.2), and our ϕ_a^2 scaling thus seemed to contradict the result of Kriesel and Driscoll. The expansion rate $\Delta \nu$, however, is related to a radial integral⁷ of the particle flux Γ , so the contradiction could not be established by measurements of Γ at a single radius. We have thus expanded our range of measurements to resolve this issue. Although the results are generally in agreement with those previously reported, we have observed some cases where the low amplitude scaling is closer to ϕ_a^1 . Both the ϕ_a^2 and ϕ_a^1 cases, however, have rigidities less than 10. Instead, we find that the ϕ_a^1 cases are characterized by an induced flux that is comparable in magnitude but opposite in sign to the background flux.

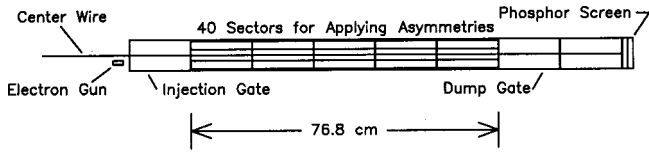


FIG. 1. Schematic of the Occidental trap. The usual plasma column is replaced by a biased wire that maintains the basic dynamical motions of low density injected electrons. The low density and high temperature of the injected electrons largely eliminates collective modifications of the vacuum asymmetry potential. The 40 wall sectors allow for the application of asymmetries consisting of essentially one Fourier mode.

II. EXPERIMENTAL RESULTS

Our experiments are performed in the modified Malmberg–Penning trap shown in Fig. 1. A thin biased wire (0.356 mm diam) running along the axis of the trap provides the radial electric field usually produced by the non-neutral plasma column. Low density electrons injected into this device have the same dynamical motions as those in a normal non-neutral plasma (i.e. axial bounce and azimuthal drift motions), but collective contributions to the asymmetry potential are largely eliminated since the lower density (10^5 cm^{-3}) and higher temperature (4 eV) of the electrons give a Debye length larger than the trap radius. This is important because the plasma response to applied wall potentials can be nonlinear, thus confusing studies of the transport scaling. The asymmetry potential within the confinement region of our trap is essentially the vacuum potential and we need not be concerned with plasma modifications of the asymmetry potential. Despite these changes in the plasma parameters, the confinement time scaling with no applied asymmetries¹⁰ shows the same $(L/B)^2$ dependence found in higher density experiments,^{11,12} thus supporting the notion that the asymmetry-induced transport is a single particle effect.

The confinement region of our trap is divided into 40 wall sectors (five axial divisions, each with eight azimuthal divisions) and these are used to produce the applied asymmetry. We use ac voltages at a variable frequency f since this gives us an additional experimental parameter that can be varied independently of other quantities. By judiciously selecting the amplitude and phase of the signal applied to each sector we can produce an asymmetry consisting of essentially a single Fourier mode, thus eliminating the sum over modes in the transport theory⁹ and making for a simpler comparison between theory and experiment. For these experiments we produce a helical standing wave with axial and azimuthal mode numbers equal to 1. The dominant asymmetry potential is thus given, to good approximation, by

$$\phi(r, \theta, z, t) = \phi_a \frac{r}{R} \cos\left(\frac{\pi z}{L}\right) \cos(\theta - \omega t),$$

where ϕ_a is the asymmetry potential at the wall, R is the wall radius (3.82 cm), L is the length of the confinement region (76.8 cm), $\omega = 2\pi f$, and z is measured from one end of the confinement region.

Electrons are injected into the trap from a 2.54 mm diameter gun at $r = 1.65$ cm, but are quickly dispersed into an annular distribution.¹³ In these experiments, the electrons are

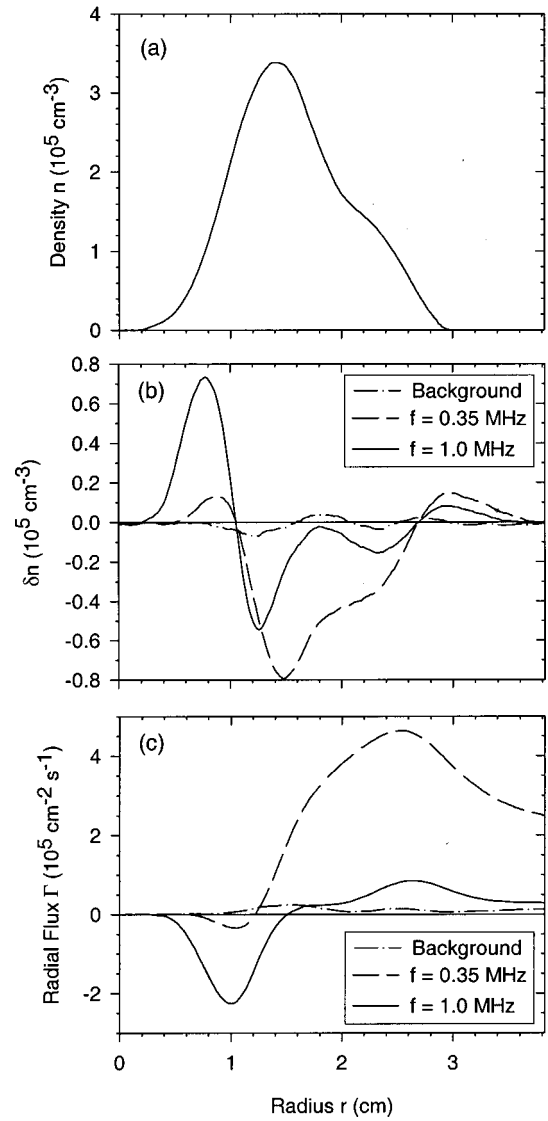


FIG. 2. Sample data showing (a) a typical density profile n , (b) the change in density due to asymmetries δn , and (c) the calculated radial flux Γ vs radial position r . The asymmetry frequencies are chosen for their ability to produce transport at different radii.

held for 1600 ms at which point the asymmetry is switched on for a variable length of time. At the end of an experimental cycle the asymmetry is switched off and the electrons are dumped onto a phosphor screen. The resulting image is digitized with a cooled charge-coupled device camera. A radial cut through this image gives the axially-integrated density profile $n(r, t)$ of the electrons. Sample data are given in Fig. 2 to orient the reader. The density profile taken 1600 ms after injection is shown in Fig. 2(a). The electrons form an annulus centered on the center wire and are broadly distributed in radius. To show the character of the radial transport we apply an asymmetry with $\phi_a = 0.2$ V for $\delta t = 100$ ms and show the resulting change in density δn for two asymmetry frequencies in Fig. 2(b). The background change in density (with no applied asymmetry) is also shown for comparison. This δn data can then be integrated to give the radial flux Γ ,

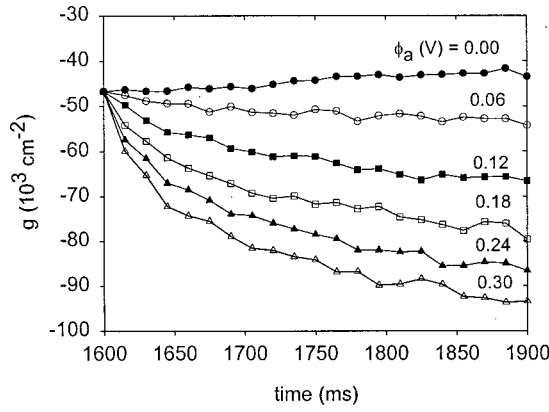


FIG. 3. A typical data set showing the computed quantity $g(r, t)$ vs time with asymmetry amplitude as a parameter. The slope of these curves gives the radial flux $\Gamma = dg/dt$. Here $r = 1.02$ cm and $f = 1.0$ MHz.

$$\Gamma(r, t) = -\frac{1}{r} \int_0^r r' dr' \cdot \frac{\delta n(r', t)}{\delta t}$$

as shown in Fig. 2(c). Note that the induced transport is quite different for $f = 0.35$ MHz and 1.0 MHz and that both inward ($\Gamma < 0$) and outward ($\Gamma > 0$) fluxes are observed. The frequency dependence of the transport is believed to be evidence for the dominance of the transport by resonant particles.⁵ For this paper, however, we are using these two frequencies simply to exploit their ability to produce appreciable transport at different radii (small radii for $f = 1.0$ MHz and larger radii for $f = 0.35$ MHz).

For this study it is useful to take density profiles at various times and then to numerically integrate the density to obtain the quantity $g(r, t)$:

$$g(r, t) = -\frac{1}{r} \int_0^r r' dr' \cdot n(r', t).$$

The time derivative of $g(r, t)$ then gives the radial particle flux $\Gamma(r, t) = dg/dt$. Figure 3 shows a typical set of data. The quantity $g(r, t)$ is plotted vs the time after injection for various asymmetry amplitudes. Here $r = 1.02$ cm and $f = 1.0$ MHz. A line is then fit to the initial slope of these curves to obtain the radial flux. This method produces less error than calculating the flux from δn taken at one time. Note that, at the higher amplitudes and later times, the slope changes as the initial plasma is modified by the transport. Plotting the data in this way thus also allows us to note and avoid these saturated cases. Finally, note that the flux is not zero for zero applied asymmetry, i.e., there is a positive background flux Γ_0 , and that the asymmetry-induced flux at this radius is negative [cf. Fig. 2(c)].

Figure 4 shows the magnitude of the net induced flux $\Delta\Gamma = |\Gamma_{\text{induced}} - \Gamma_0|$ vs asymmetry amplitude ϕ_a with radial position as a parameter. The experimental conditions are similar to those of Ref. 5, Fig. 3 (center wire bias = -80 V, $B = 365$ G, $f = 1$ MHz). The log-log plot allows us to determine the scaling exponent m , where $\Delta\Gamma \propto \phi_a^m$. Typical error bars are shown, and lines of slope one and two are drawn for comparison to the data. The results are similar to those reported in Ref. 5: the net flux scales roughly like ϕ_a^2 for low

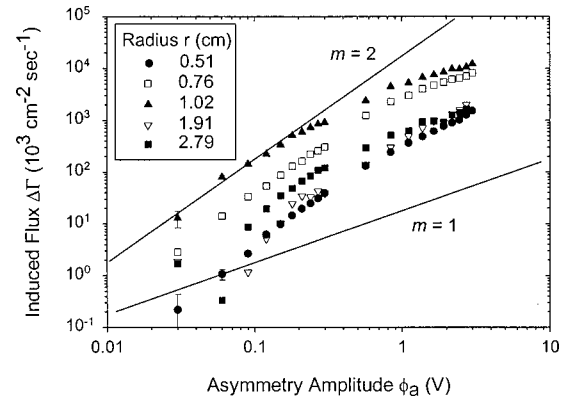


FIG. 4. Log-log plot of the net asymmetry-induced flux $\Delta\Gamma$ vs the applied asymmetry amplitude at the wall ϕ_a with radial position r as a parameter. The asymmetry frequency f is 1 MHz. Lines of slope one and two are shown for comparison. For the cases shown the low amplitude scaling is close to ϕ_a^2 .

amplitude asymmetries, in agreement with plateau-regime theory. At higher amplitudes, the scaling exponent falls off to a smaller value in the range 0.5 to 1.4. This may indicate a transition to banana-regime scaling $\phi_a^{1/2}$, but the data is not sufficient to support this conclusion. Note that there is no dramatic dependence of m on radius, so if we were to calculate the expansion rate $\Delta\nu$ as in Ref. 8 the low amplitude scaling would still be ϕ_a^2 .

Exploration of our parameter space has found some cases showing scaling closer to ϕ_a^1 and some of these cases are shown in Fig. 5. For these parameters (as above except $f = 0.35$ MHz), the ϕ_a^1 cases occur at smaller radii while ϕ_a^2 cases occur at larger radii. Again, a calculation of expansion rate would not yield a ϕ_a^1 scaling. Cases showing a ϕ_a^1 scaling also occur for $f = 1.0$ MHz for radii near 1.4 cm (not shown in Fig. 4 for clarity). The appearance of ϕ_a^1 scaling is thus not due to the change of frequency.

Kriesel and Driscoll found that their amplitude scaling regimes were correlated with rigidity, with the ϕ_a^2 cases occurring for rigidities greater than 10 and ϕ_a^1 cases for rigidities less than 10. To test this correlation, in Fig. 6 we plot the scaling exponent m versus the rigidity for the cases we have

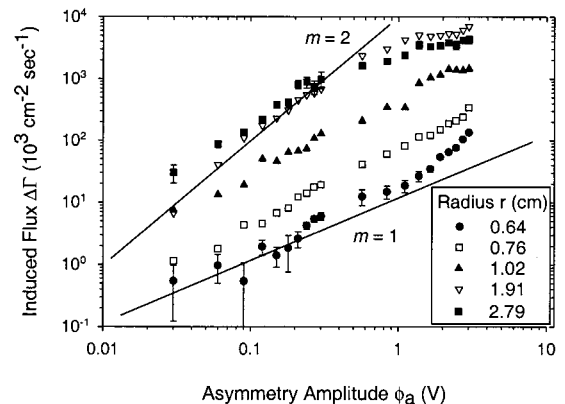


FIG. 5. Log-log plot of the net asymmetry-induced flux $\Delta\Gamma$ vs the applied asymmetry amplitude at the wall ϕ_a for $f = 0.35$ MHz. For the lower radii the scaling exponent is close to 1.

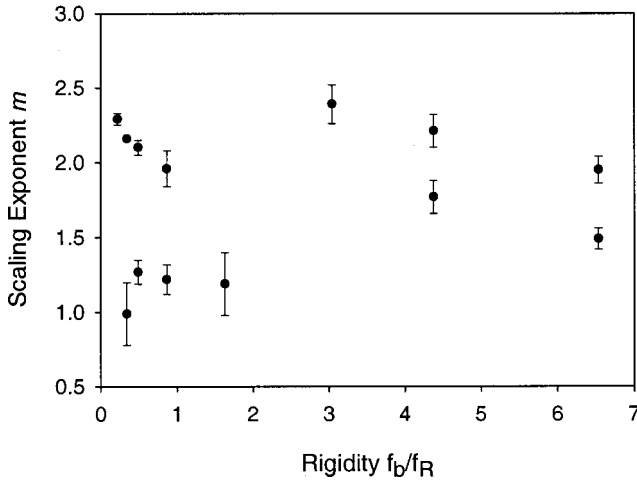


FIG. 6. Scaling exponent m vs rigidity. No correlation is observed with this parameter.

considered. Note that all these cases have rigidity less than 10 (the borderline value for the Kriesel–Driscoll regimes), and, more importantly, that the same value of rigidity gives both $m \approx 1$ and $m \approx 2$ cases. Thus, in our experiment the scaling exponent is not correlated with rigidity.

We have tried to find correlation with other parameters as well. Since our experiments use a nonzero asymmetry frequency f , it might make sense that the rigidity should be modified from f_b/f_R to $f_b/(f-f_R)$ since presumably this ratio measures rigidity relative to the asymmetry. A plot of the data, however, shows no correlation of the scaling exponent with this modified rigidity either. Other quantities that fail to correlate with m include $f-f_R$, $(f-f_R)/f_R$, Γ_0 , and Γ_{induced} .

A re-examination of the original data for the $m=1$ cases shows typical g vs t plots like the one shown in Fig. 7. Here $r=0.76$ cm and $f=0.35$ MHz. For these cases, the background flux is comparable in magnitude to the induced flux. Following this clue, we have plotted in Fig. 8 the scaling

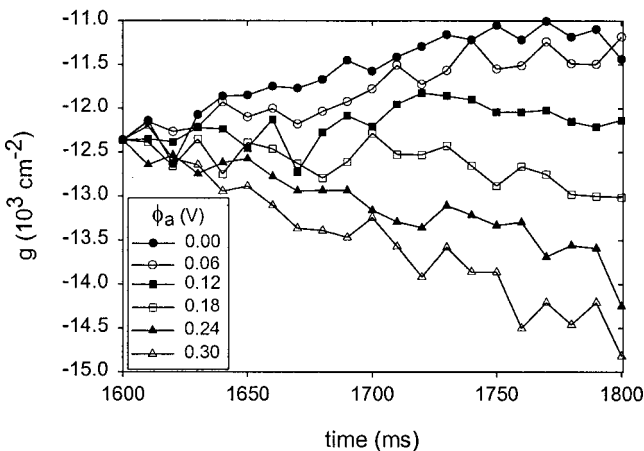


FIG. 7. Typical g vs t data for cases yielding a scaling exponent near 1. The magnitude of the background transport is comparable to that of the induced transport. Here $r=0.76$ cm and $f=0.35$ MHz.

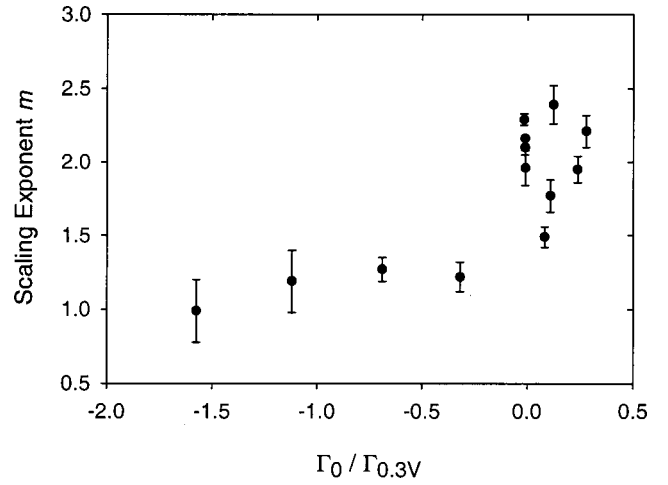


FIG. 8. The scaling exponent m shows a correlation with the ratio of the background flux Γ_0 to a typical induced flux $\Gamma_{0.3V}$.

exponent vs the ratio of the background flux to the induced flux at a typical asymmetry value of 0.3 V. The correlation here is good, with $m=2$ cases corresponding to smaller values of $\Gamma_0/\Gamma_{0.3V}$ and the $m=1$ cases corresponding to larger negative values.

III. DISCUSSION

The fact that our $m=1$ cases occur when the background flux is comparable in magnitude to the induced flux suggests a simple mixing of applied and background asymmetries. Suppose that the true flux scaling is $\Gamma \propto \phi_a^2$ and that when both a background asymmetry ϕ_0 and an applied asymmetry ϕ_a are present they add directly. The total asymmetry squared is then $\phi_a^2 + 2\phi_a\phi_0 + \phi_0^2$, and if $\phi_a \ll \phi_0$, we obtain $\Gamma - \Gamma_0 \propto \phi_a$. Such a model, however, is not consistent with the details of the experimental data or with the theory. At least one experimental case where the flux scales like ϕ_a^1 occurs in the middle of our plasma ($r=1.4$ cm, $f=1.0$ MHz) with ϕ_a^2 cases at smaller and larger radii. The above model would then require a background asymmetry that is peaked in the middle of the plasma and it is hard to imagine how such an asymmetry could be produced. This direct addition model is also inconsistent with the theory, which says the flux is given by a sum of terms, one for each Fourier mode produced by the asymmetries. In our case, the background asymmetry is static (i.e., zero frequency) while the applied asymmetry has a nonzero frequency. These will necessarily give different Fourier modes that, according to the theory, should not add directly. It would seem that the explanation for our observed correlation must be at a deeper level than simple addition of asymmetry potentials.

It has been suggested¹⁴ that the ϕ_a^1 scaling is due to the large size of the asymmetries employed in some experiments. In these cases the small-perturbation assumption of the quasilinear theory is violated. If the applied asymmetry is large enough ($e\phi \gg kT$), particles will be excluded from (or pulled into) the vicinity of the biased wall sector. The perturbation of the distribution function δf would thus be large and saturated (i.e., no longer dependent on the perturbed po-

tential in the plasma $\delta\phi$). Since the transport goes like the product $\delta f \delta\phi$, the dependence would be linear in the asymmetry amplitude. While this model might explain some experimental results (for example, the fall-off of our scaling exponent with asymmetry amplitude), it does not seem consistent with the bulk of the data, either in our experiments or those of others. For example, when we observe ϕ_a^1 scaling, it is observed even at very low asymmetry amplitudes. In contrast, Notte and Fajans observed ϕ_a^2 scaling even at extremely high asymmetry potentials. It is also not understood why this model should depend on rigidity, so it cannot explain the two scaling regimes observed by Kriesel and Driscoll.

It is interesting to ask whether the Kriesel–Driscoll results can be explained in terms of our findings. From the data in Ref. 7, it appears that the ϕ_a^1 scaling does occur for cases where the induced transport is comparable to the background transport. The ϕ_a^2 cases are harder to judge because the background transport was so small it was taken to be zero. Although this would fit into our scheme (i.e., $\Gamma_0/\Gamma_{\text{induced}}$ would be zero), a more careful measurement would be required to settle this question.

IV. CONCLUSION

We find that in most cases the asymmetry-induced transport in our experiment produces a net radial flux that scales like the square of the applied asymmetry amplitude for small asymmetries and falls off to a weaker dependence (m

$=0.5-1.4$) for larger amplitudes. We have found some cases that give a low-amplitude scaling exponent closer to 1. These cases are not correlated with rigidity as in Ref. 8 but occur when the induced flux is comparable in magnitude but opposite in sign to the background flux. We do not yet understand the reason for this correlation.

ACKNOWLEDGMENTS

This work was supported by U.S. Department of Energy Grant No. DE-FG03-98ER54457. Summer stipend for B.C. was provided by NSF–CAMP.

- ¹J. H. Malmberg and C. F. Driscoll, Phys. Rev. Lett. **44**, 654 (1980).
- ²D. L. Eggleston, T. M. O’Neil, and J. H. Malmberg, Phys. Rev. Lett. **53**, 982 (1984).
- ³J. Notte and J. Fajans, Phys. Plasmas **1**, 1123 (1994).
- ⁴X.-P. Huang, F. Anderegg, E. M. Hollman, C. F. Driscoll, and T. M. O’Neil, Phys. Rev. Lett. **78**, 875 (1997).
- ⁵D. L. Eggleston, in *Non-Neutral Plasma Physics III*, edited by J. J. Bollinger, R. L. Spencer, and R. C. Davidson (American Institute of Physics, Melville, NY, 1999), p. 241.
- ⁶J. M. Kriesel and C. F. Driscoll, in Ref. 5, p. 256.
- ⁷J. M. Kriesel, Ph.D. thesis, University of California San Diego, 1999.
- ⁸J. M. Kriesel and C. F. Driscoll, Phys. Rev. Lett. **85**, 2510 (2000).
- ⁹D. L. Eggleston and T. M. O’Neil, Phys. Plasmas **6**, 2699 (1999).
- ¹⁰D. L. Eggleston, Phys. Plasmas **4**, 1196 (1997).
- ¹¹C. F. Driscoll and J. H. Malmberg, Phys. Rev. Lett. **50**, 167 (1983).
- ¹²C. F. Driscoll, K. S. Fine, and J. H. Malmberg, Phys. Fluids **29**, 2015 (1986).
- ¹³D. L. Eggleston, Phys. Plasmas **1**, 3850 (1994).
- ¹⁴T. M. O’Neil (private communication, 2001).